

Study on the Impact Factor of Recycled Asphalt Concrete Bridge Pavement

Fang Wang , Zhengzheng Chen

Abstract—The use of recycled asphalt concrete pavement (RACP) is becoming increasingly prevalent due to its significant contribution to the conservation of raw materials for pavement. The recycled asphalt concrete' (RAC) physical and mechanical properties have been extensively studied. However, there is an urgent need to verify its ability to withstand dynamic loads. The impact factor (*IM*) represents a crucial criterion for measuring the bridge structures' dynamic responses. In this study, the *IMs* of RACP and ordinary asphalt concrete pavement (OCP) were calculated by a three-dimensional (3D) vehicle-bridge coupled model that have been validated before. A comparison was made between the calculated *IMs* and the values specified in two specifications, the AASHTO (2020) LRFD code and the Chinese bridge design specification (JTG D60-2015). Furthermore, the *IMs* were studied in relation to the initial vehicle speed, road surface condition (RSC) and different vehicle truck models. The results demonstrated that the *IMs* of the RACP could meet the requirements of AASHTO (2020) and JTG D60-2015 under normal traffic conditions.

Index Terms—Recycled asphalt concrete pavement(RACP), Ordinary asphalt pavement(OAP), Impact factor(*IM*), Bridge code.

I. INTRODUCTION

CURRENTLY, the construction of high-grade roads in China is primarily focused on renovation and expansion, as well as major maintenance. This process generates a significant amount of asphalt pavement waste [1,2]. The efficient and environmentally friendly recycling of this pavement waste is a key research focus and will continue to be in the future [3,4].

The pavement made by removing and reprocessing pavement materials containing asphalt and other aggregates is recycled studies have focused on the basic physical properties of recycled concrete aggregate asphalt concrete pavement (RACP). Due to the increasing acceptance of RACP in the construction industry, it has been widely studied in various areas, such as bridge pavement applications [5].

In the past, , including elastic modulus and compressive

strength [6,7]. Huang et al. [5] conducted laboratory experiments with the objective of investigating the mechanical properties of silicate cement concrete when incorporated with RACP, the results showed that the energy absorption toughness for the RACP-incorporated concrete was significantly increased. Bhardwaj and Singh [8] studied the cohesion failure of RACP and found that the failure of RACP was determined by many parameters, including the mineralogy of the aggregates, and the characteristics of the cement-mortar paste, and the asphalt aging intensity. Their research results also indicated that the failure mechanism of RACP was a function of all the variations studied. Rafiq et al. [9] studied the effects of using crude palm oil in hot-mix asphalt incorporating RACP. The findings of their study demonstrated that the stability and indirect tensile strength of RACP material increased up to 80% with increasing the content of RACP material.

Previous research on the RACP primarily concentrated on static performance, but there have been few studies on its dynamic responses. Okafor [10] found that recycled aggregate can absorb more impact load than conventional aggregate, which is beneficial for reducing the impact load.

It is well known that moving vehicles create greater deformation and internal forces on bridges compared with a static load, which is a pivotal element in the proper design and safe operation of bridges [11-13]. To consider the dynamic response of bridges caused by the movement of vehicle loading, the impact factor (*IM*) is generally proposed in the bridge design specifications in various countries [14-16]. In previous studies, the *IMs* of traditional bridge pavements have been studied in considerable depth. For example, a variety of analytical bridge-vehicle models have been employed in order to examine the dynamic effects of vehicle loads [17-20]. At the same time, field tests have been conducted to validate the *IMs* as stipulated in the design specifications [21-23]. Furthermore, a comprehensive study has been undertaken on the parameters that affect the *IM* [24-26].

In this paper, the dynamic performance and *IMs* of RACP were investigated by using a validated 3D vehicle-bridge coupled model. Two types of pavements, ordinary concrete pavement (OCP) and RACP, were simulated for the same bridge model. The values of *IMs* were calculated for both pavements under different working conditions. The *IMs* obtained were then subjected to comparison with the values that had been stipulated in the AASHTO (2020) LRFD code and the Chinese code. Moreover, a parametric study was conducted to explore the effect of differing parameters on *IMs*.

Manuscript received April 29, 2024; revised February 24, 2025.

This work was supported by Key Scientific Research Project of Suzhou University(2024yzd09), Investigator-the School-enterprise Cooperation project (No.2023xhx003), University Scientific Research Project of Anhui Education Department(No.2023AH052244) and Key Scientific Research Project of Suzhou University(2024yzd08).

Fang Wang is a lecturer in the Department of Resources and Civil Engineering, Suzhou University, Suzhou 234000, China (Corresponding author, phone: +8615715572606; E-mail:15715572606@163.com).

Zhengzheng Chen is a lecturer in the Department of Resources and Civil Engineering, Suzhou University, Suzhou 234000, China (Co-Corresponding author, phone: +8617719319721, E-mail:15211065545@163.com).

II. METHODS

The ANSYS software has a wealth of modeling tools, and it can quickly construct a variety of complex geometric models, perform high-precision numerical calculations, and achieve accurate simulation results. The MATLAB software provides a rich toolbox and library of functions that facilitate data processing and algorithm development. The bridge model in this paper was modeled using solid elements of ANSYS software. The *IM* calculations and data analysis were performed using the MATLAB software.

III. BRIDGE MODEL

The ANSYS software was used to model a concrete T-beam bridge using solid elements in this study. And the finite element model was demonstrated in Figure 1. The span of the bridge was 20 meters long, with a deck width of 8.5 meters, and a thickness of 0.20 meters. The structural fundamental frequency was 5.865 Hz. The load position of the vehicle and the bridge’s cross section can be seen in Figure 2, the vehicle was positioned so as to travel along the centreline of Lane 2, and the unit of length in the figure is millimeters.

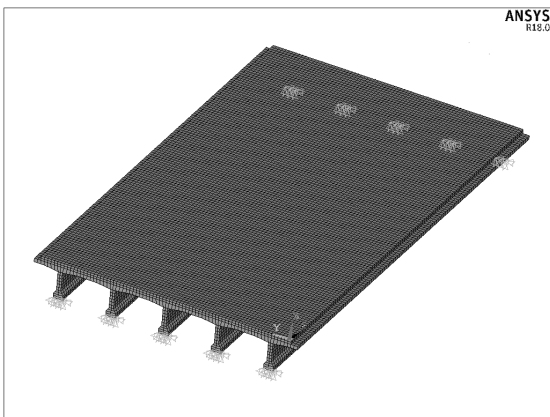


Fig. 1. Finite element model of the bridge.

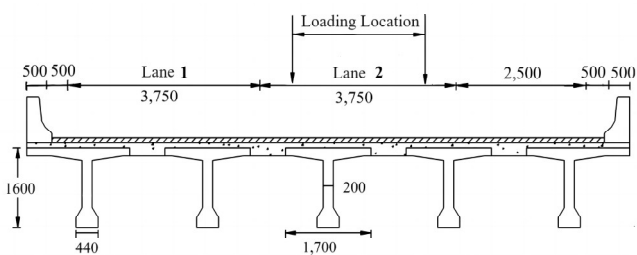


Fig. 2. The bridge cross section and the vehicle loading location.

IV. VEHICLE MODEL

In this paper, two common vehicle models as illustrated in Figures 3 and 4, were considered to compare the dynamic responses of the two pavements when different vehicles passed by. In the model, *C* and *K* are used to denote the damping and stiffness matrices of the vehicle, respectively; the motions of the vehicle in the directions of the degrees of freedom are denoted by *z* and θ ; the geometric dimension of the vehicle is denoted L_i , and *r* is the road profile.

The details of the two-axle truck were reported by Zhang et al. [27]. The three-axle truck used was the HS20-44 truck

adopted in AASHTO (2020), and its detailed properties were reported by Deng and Cai [11].

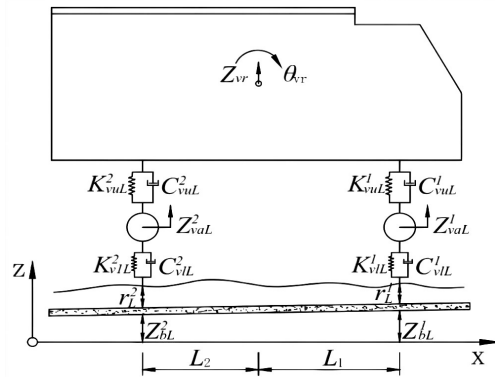


Fig. 3. 2-axle vehicle model.

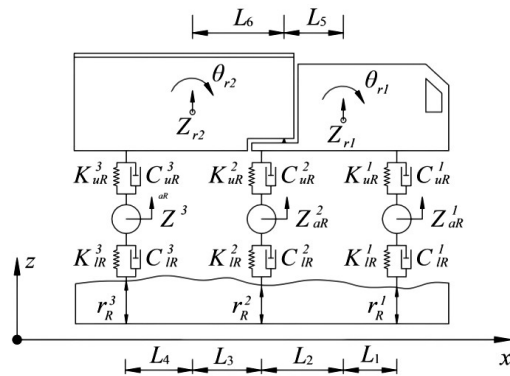


Fig. 4. 3-axle vehicle model.

V. ROAD SURFACE CONDITION

The RSC is the primary source of vibrations caused by vehicles on bridges. It can be described in terms of a power spectral function, and it is usually treated as a random process.

The International Organization for Standardization (ISO 1995) proposed a road roughness index that could be used to describe the characteristics of a road surface. The index ranges from “very good” to “very poor” as shown in Table 1. In this study, three kinds of RSCs of “good,” “average,” and “poor” were adopted.

TABLE I
RSC CLASSIFICATIONS INDEX FOR DIFFERENT ROAD SURFACE CONDITIONS

RSC classifications	Index values(m ³ /cycle)
Very good	2×10^{-6} to 8×10^{-6}
Good	8×10^{-6} to 32×10^{-6}
Average	32×10^{-6} to 128×10^{-6}
Poor	128×10^{-6} to 512×10^{-6}
Very poor	512×10^{-6} to 2048×10^{-6}

In this study, the randomness of the generated road surface profile was minimised by generating 20 random profiles and setting the coupled vehicle-bridge system to run 20 times. The average of the 20 *IMs* was then calculated for the further study.

VI. MOTION EQUATION OF COUPLED VEHICLE-BRIDGE SYSTEM

The displacement relation and the interaction between the contact points can be used to calculate the combined motion of the bridge-vehicle with the following equation:

$$\begin{bmatrix} M_b & \\ & M_v \end{bmatrix} \begin{Bmatrix} \ddot{d}_b \\ \ddot{d}_v \end{Bmatrix} + \begin{bmatrix} C_b + C_{b-b} & C_{b-v} \\ C_{v-b} & C_v \end{bmatrix} \begin{Bmatrix} \dot{d}_b \\ \dot{d}_v \end{Bmatrix} + \begin{bmatrix} K_b + K_{b-b} & K_{b-v} \\ K_{v-b} & K_v \end{bmatrix} \begin{Bmatrix} d_b \\ d_v \end{Bmatrix} = \begin{Bmatrix} F_{b-r} \\ F_{b-r} + F_G \end{Bmatrix} \quad (1)$$

where the subscripts b , v , and r are used to denote “bridge,” “vehicle”, and “road roughness”, respectively; M , C , and K represent the mass, damping, and stiffness matrices, respectively; d represents displacement; F_G is the force of gravity acting on the vehicle; It should be noted that the subscripts $b-b$, $b-v$, $v-b$ and $b-r$ represent time-dependent parameters that are associated with vehicle-bridge interactions.

The method of Runge-Kutta algorithm in the time domain can be used to solve Equation (1). More details of the solution process and the further details on the construction of coupled systems in vehicles and bridges were reported by Deng and Cai [11].

VII. DEFINITION OF IMPACT FACTOR IN BRIDGE CODES

A. Definition of the Impact Factor

The impact factor(IM) is a factor to amplify the static load by considering the dynamic effect produced when the vehicle is traveling, which is typically calculated using the following formula:

$$IM = \frac{y_{dmax}}{y_{smax}} - 1 \quad (2)$$

where y_{dmax} and y_{smax} represent the maximum dynamic and static responses of the bridge, respectively. The responses of a bridge can be calculated from the displacement, strain, and reaction force in the numerical simulations. In this paper, the bridge’s maximum vertical displacement and strain responses under vehicle loads were selected for the purpose of calculating IM . The vehicle was set to cross the bridge with a velocity of 0.5 m/s in order to achieve the maximum static response in the ANSYS program. It should be noted that the values of IM obtained by different responses were not necessarily the same [18,22].

B. AASHTO Code

TABLE II
IMPACT FACTORS (IM s) IN AASHTO (2020)

Component	Limit state	IM
Deck joint	All limit states	0.75
All other components	Fatigue and fracture limit states	0.15
	All other limit states	0.33

The AASHTO (2020) LRFD code takes the category and calculation status of the component as the main consideration to determine the impact effect. Because the joints are the weak part of the bridge and the force transfer effect decreases

rapidly, the IM at the joint has a larger value of 0.75, which is conducive to ensuring the safety of the joint and the integrity of the structure. It is more appropriate to use a smaller value for fatigue checks. The specific values are given in Table 2.

C. Chinese Code

The fundamental frequency of the bridge structure comprehensively reflects the type, size, construction materials, and other dynamic characteristics of the structure. Therefore, the Chinese bridge design code JTG D60-2015 stipulates that IM is a function of fundamental frequency as follows:

$$\begin{cases} IM = 0.05, & f < 1.5Hz; \\ IM = 0.1767 \ln f - 0.0157, & 1.5Hz < f < 14Hz; \\ IM = 0.45, & f > 14Hz \end{cases} \quad (3)$$

where f denote the fundamental frequency of the bridge.

VIII. PARAMETRIC STUDY

In this study, the IM s were calculated by the displacements and strains at the mid-span of the girder subjected to the maximum vehicle load. The calculated results were then compared with the AASHTO (2020) and JTG D60-2015 values under certain working conditions. Finally, the effects of three different parameters, including the initial vehicle speed, road surface condition, and vehicle model, on the IM s of the two pavement types were investigated. Specifically, the examined parameters were as follows: (1) three kinds of RSCs, namely “good”, “average”, and “poor”; (2) five initial vehicle speeds, namely 10 m/s, 15m/s, 20m/s, 25m/s and 30 m/s; (3) two types of pavements, namely OCP and RACP; (4) 2-axle and 3-axle trucks.

A. Comparison with Values Specified in Bridge Code

To compare the relationships between the IM s of the two road pavements and the standard values in the bridge codes, the results obtained by the two-vehicle models under the same working conditions at a speed of $v=20$ m/s are shown in Table III. In addition, the calculated IM s were then subjected to comparison with the values stipulated by AASHTO (2020) and JTG D60-2015.

From Table 3, the followings can be found: (1) For the two-vehicle models used in this paper, the IM s of the three-axle heavy vehicle model were smaller than those of the two-axle light vehicle under the same conditions, which is consistent with findings in other studies that the IM decreased as the static load effect increased. (2) For OCP, the IM s of the three-axle vehicle were less than the IM s specified in both AASHTO (2020) and JTG D60-2015 under the three types of RSC. For the RACP, the IM s caused by the three-axle vehicle were found to be less than those stipulated in both AASHTO (2020) and JTG D60-2015 when the RSCs were “good” and “average.” In fact, it is when the pavement condition is “poor” that road maintenance work needs to be carried out. It can be seen that the pavement made with the waste asphalt mixture met the design and use requirements to a certain extent. (3) In addition, it can be seen that under the same working condition, the IM s calculated by the deflection response were smaller than those calculated by the strain for both bridge pavements.

TABLE III
IMs OF TWO KINDS OF PAVEMENT AND COMPARISON WITH THE STANDARD VALUES

Vehicle model	RSC	IM (DEFLECTION)		IM (STRAIN)		IMs IN BRIDGE CODES	
		OCP	RACP	OCP	RACP	AASHTO (2020)	JTG D60-2015
2-axle vehicle truck model	good	0.141	0.159	0.117	0.131		
	average	0.274	0.317	0.212	0.255		
	poor	0.513	0.557	0.441	0.47		
3-axle vehicle truck model	good	0.073	0.081	0.071	0.077	0.297	0.330
	average	0.152	0.166	0.149	0.154		
	poor	0.293	0.317	0.287	0.300		

B. Effect of Vehicle Initial Speed and RSC

To compare the relationships between the IM, speed, and RSC, the IMs with five initial speeds under the three types of RSC were calculated for the 3-axle vehicle model for both the OCP and RACP. The results can be seen in Figure 5, where Figures 5 (a) and (b) show the IMs calculated by the deflection response and strain response, respectively.

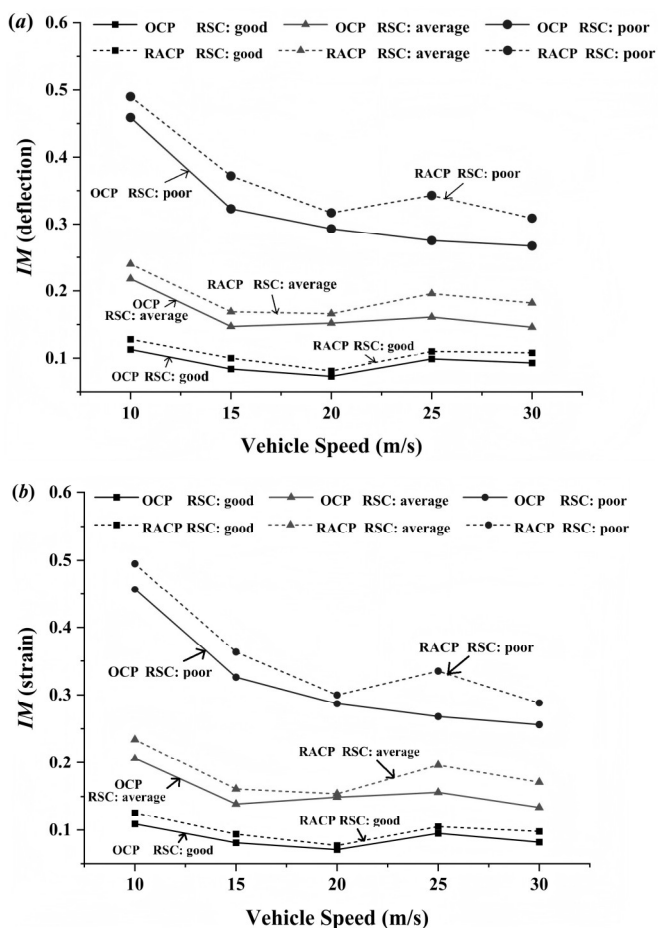


Fig. 5. IMs under different vehicle speeds and RSCs: (a) from deflection (b) from strain.

From Figure 5, the followings can be seen for the same working conditions: (1) The IMs calculated by the RACP were slightly larger than those of the OCP, indicating that the impact resistance of the RACP was likely to meet the design and application requirements. (2) The trend of the RACP’s IMs with initial vehicle speed was not so significant, which is

in general accordance with the OCP results as reported in other studies. In addition, we can see that vehicle speed was one of the main factors affecting IM. With the other parameters equal, different vehicle speeds resulted in very different IMs. (3) The effect of condition of the RSC on the IMs was significant. Typically, the IMs increased significantly with the deterioration of the RSC. (4) The difference between the IM values calculated from the deflection response and the strain response was very small, and the variation trend with the vehicle speed was basically the same.

C. Effect of different Vehicle Models

To compare the effects of different vehicle models on the IMs of the two types of pavements, the IMs obtained from deflection responses of the 3-axle and 2-axle vehicles were calculated for both the OCP and RACP. It should be noted that the IMs reported here are the average values of the IMs obtained at the five speeds to avoid the deviations caused by a single velocity value. The results are shown in Figure 6.

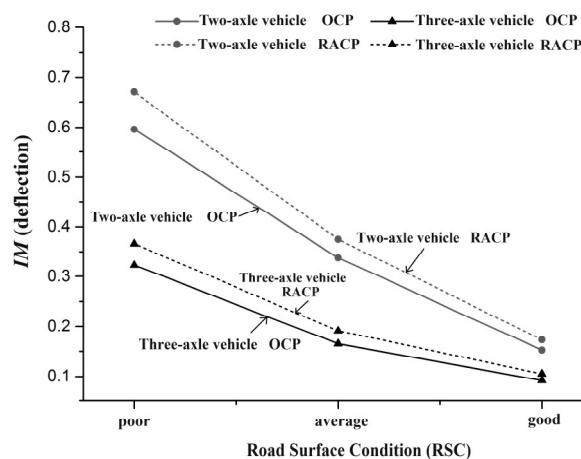


Fig. 6. IMs for two different vehicle truck models.

As illustrated in Figure 6: (1) Under the same conditions, the IMs of the 2-axle vehicle were larger than those of the 3-axle vehicle for both the RACP and OCP. (2) The IM was significantly influenced by the RSC. When the RSC changed from “poor” to “average” and “good”, the values of the IM showed a clear linearly decreasing trend. Therefore, it is essential to perform timely maintenance of the road surface in actual bridge operation to reduce the impact of vehicles and ensure the safety of the bridge.

IX. CONCLUSIONS

In this paper, the *IMs* of RACP and OCP were calculated using a 3D vehicle-bridge model. A comparison was made between the calculated *IMs* and the values stipulated in both AASHTO (2020) and JTG D60-2015. The following key conclusions can be drawn:

1) For the RACP, the *IMs* generated by the 3-axle vehicle were less than the values specified in the both specifications when the RSCs were “good” and “average”, indicating that the RACP could meet the design and use requirements.

2) With all parameters equal, the *IMs* of the RACP were slightly larger than those of the OCP, but in most cases, the value of *IMs* did not exceed the values specified in the two specifications.

3) The *IMs* of the two types of bridge pavement followed similar trends as the initial speed varied, and both exhibiting an increase in conjunction with a deterioration in the road surface conditions.

4) Under the same conditions, the *IMs* of the two-axle vehicle were found to be larger than those of the three-axle vehicle for both types of bridge pavement. This is consistent with previous studies, but it does not provide greater practical guidance, as the corresponding total load effect in this case was still small.

It should be noted that this study is mainly conducted by simulation and analysis. Due to the complexity of materials, relevant experimental studies should be carried out in the future to verify the conclusions in this paper.

REFERENCES

[1] Thives LR, Ghisi E, “Asphalt mixtures emission and energy consumption: A review,” *Renewable and Sustainable Energy Reviews*, vol. 72, pp. 473-484, 2017.

[2] Bastidas-Martínez JG, Reyes-Lizcano FA, Rondón-Quintana HA, “Use of recycled concrete aggregates in asphalt mixtures for pavements: A review,” *Journal of Traffic and Transportation Engineering (English Edition)*, vol. 9, no. 5, pp. 725-741, 2022.

[3] Victory, W., “A review on the utilization of waste material in asphalt pavements”. *Environ Sci Pollut Res*, no. 29, pp. 27279–27282, 2022.

[4] Salehi S., Arashpour M., Kodikara J., *et al.* “Sustainable pavement construction: A systematic literature review of environmental and economic analysis of recycled materials,” *Journal of Cleaner Production*, no. 33, p. 127936, 2021.

[5] Huang BS, Shu X, Li GQ, “Laboratory investigation of portland cement concrete containing recycled asphalt pavements,” *Cement and Concrete Research*, vol. 35, no. 10, pp. 2008-2013, 2005.

[6] Liu, S., Zhang, Z., Wang, R, “Performance Evaluation of Asphalt Concrete Incorporating Steel Slag Powder as Filler under the Combined Damage of Temperature and Moisture,” *Sustainability*, vol. 15, no. 19, p. 1465315, 2023.

[7] Karthikeyan K, Kothandaraman S, Sarang G, “Perspectives on the utilization of reclaimed asphalt pavement in concrete pavement construction: A critical review,” *Case Studies in Construction Materials*, vol. 19, p. e02242, 2023.

[8] Bhardwaj BB, Singh S, “Evaluation of the failure planes in concrete containing reclaimed asphalt pavement (RAP) aggregates.” *Cement and Concrete Composites*, vol. 145, p. 105334, 2024.

[9] Rafiq W, Napiyah M, Habib NZ, *et al.* “Modeling and design optimization of reclaimed asphalt pavement containing crude palm oil using response surface methodology,” *Construction and Building Materials*, no.291, p. 123288, 2021.

[10] Okafor F O, “Performance of recycled asphalt pavement as coarse aggregate in concrete,” *Leonardo electronic journal of practices and technologies*, vol. 17, pp. 47-58, 2010.

[11] Deng L, Cai C S., “Development of dynamic impact factor for performance evaluation of existing multi-girder concrete bridges,” *Engineering Structures*, vol. 32, no. 1, pp. 21-31, 2010.

[12] Zhang WM, Chang JQ, Lu XF, *et al.* “Suspension bridge deformation and internal forces under the concentrated live load: Analytical algorithm,” *Engineering Structures*, vol. 248, p. 113271, 2021.

[13] Kyosuke Yamamoto, “Experimental Study about the Applicability of Traffic-induced Vibration for Bridge Monitoring.” *Engineering Letters*, no. 2, pp.276-280, 2018.

[14] General Specifications for Design of Highway Bridges and Culverts (JTG 2015), Ministry of Transport of the People’s Republic of China (MTPRC), Beijing.

[15] AASHTO LRFD bridge design specifications, AASHTO, Washington, DC, 2020.

[16] British Standards Institution (BSI). “Steel, concrete and composite bridges,” Part 2: Specification for loads. BS 5400-2, London, 2006.

[17] Zhang Y, Cai C S, Shi X, *et al.* “Vehicle-induced dynamic performance of FRP versus concrete slab bridge,” *Journal of Bridge Engineering*, vol. 11, no. 4, pp. 410-419, 2006.

[18] Azimi H, Galal K, Pekau OA. “A modified numerical VBI element for vehicles with constant velocity including road irregularities,” *Engineering Structures*, vol. 33, no. 7, pp. 2212-2220, 2011.

[19] Zhong H, Yang MJ, Gao ZL, “Dynamic responses of prestressed bridge and vehicle through bridge-vehicle interaction analysis,” *Engineering Structures*, vol. 87, pp. 116-125, 2015.

[20] Qin SQ, Feng JC, Zhou YL, *et al.* “Investigation on the dynamic impact factor of a concrete filled steel tube butterfly arch bridge,” *Engineering Structures*, vol. 252, p. 113614, 2022.

[21] Shi XM, “Structural performance of approach slab and its effect on vehicle induced bridge dynamic response,” Ph.D. dissertation. Baton Rouge (LA): Louisiana State University, 2006.

[22] Law SS, Zhu XQ, “Bridge dynamic responses due to road surface roughness and braking of vehicle,” *Journal of Sound and Vibration*, vol. 282, no. 3-5, pp. 805-830, 2005.

[23] Guo AX, Liu JB, Chen WL, *et al.* “Experimental study on the dynamic responses of a freestanding bridge tower subjected to coupled actions of wind and wave loads,” *Journal of Wind Engineering and Industrial Aerodynamics*, vol. 159, pp. 36-47, 2016.

[24] Majka M, Hartnett M, “Effects of speed, load and damping on the dynamic response of railway bridges and vehicles,” *Computers & Structures*, vol. 86, no. 6, pp.556-572, 2008.

[25] Huang PM, Wang JF, Han WS, *et al.* “Study on impact factors of small- and medium-span bridges under the special-purpose vehicle load,” *Structures*, vol. 43, pp. 606-620, 2002.

[26] Brady, Sean P, O'Brien E, *et al.* “The Effect of Vehicle Velocity on the Dynamic Amplification of a Vehicle crossing a Simply Supported Bridge,” *Journal of Bridge Engineering*, vol. 11, no. 2, pp. 137-138, 2017.

[27] Zhang Y, Cai C S, Shi, X, *et al.* “Vehicle-induced dynamic performance of FRP versus concrete slab bridge,” *Journal of Bridge Engineering*, vol. 11, no. 4, pp. 410-419, 2006.

[28] ISO 8068, “Mechanical vibration-Road surface profiles-reporting of measured data,” Geneva, pp. 18-24, 1995.

[29] Ashebo DB, Chan TH, Yu L, “Evaluation of dynamic loads on a skew box girder continuous bridge Part II: Parametric study and dynamic load factor,” *Engineering Structures*, vol. 29, no. 6, pp. 1064-1073, 2007.

[30] Heng K, Li RW, Li ZR, *et al.* “Dynamic responses of highway bridge subjected to heavy truck impact,” *Engineering Structures*, vol. 232, p. 111828, 2021.